American Journal of Science and Technology
2014; 1(4): 168-181
Published online August 30, 2014 (http://www.aascit.org/journal/ajst)

American Association for Science and Technology


**Keywords**
Injection Over-Molding, Polymer-Metal Hybrid (PMH) Technologies and Structures, Automotive Structural Components

Received: August 22, 2014
Revised: August 27, 2014
Accepted: August 28, 2014

# Injection over molding of polymer-metal hybrid structures

**M. Grujicic**

Department of Mechanical Engineering, Clemson University, Clemson SC 29634, USA

## Email address

gmica@clemson.edu

## Citation

M. Grujicic. Injection Over Molding of Polymer-Metal Hybrid Structures. *American Journal of Science and Technology.* Vol. 1, No. 4, 2014, pp. 168-181.

## Abstract

A comprehensive overview is provided of the key aspects of injection over-molding technologies used in automotive body-in-white (BIW) structural applications. Specifically, the following aspects of injection-molding technologies are discussed: (a) fundamental concepts related to synergistic polymer/metal interactions; (b) classification of the technologies; (c) basics of polymer/metal adhesion and load transfer; (d) application of computational engineering methods and tools for process and product-performance simulations; and (e) compatibility of different injection-molding PMH technologies with the automotive BIW manufacturing process chain.

## 1. Introduction

In the traditional automotive manufacturing practice, a choice has to be typically made between the use of metals and plastics for various structural and non-structural applications. This paradigm is gradually being shifted with the introduction of Polymer Metal Hybrid (PMH) structures in which metals and polymers are integrated in a singular component/sub-assembly. The main motivation behind the introduction of the PMH technology into the automotive manufacturing practice is to, through the application of a system-level approach, combine various requirements of several adjacent components into a singular component/sub-assembly (typically consisting of a metal-stamping core and plastic injection-molded overcoat containing multiple ribs) in order to deliver a customer-specific solution/function [1–10]. When metals and polymers are successfully integrated into a single component/sub-assembly, the system-level benefits obtained are greater than those attained through simple merging/joining of the proximal parts. In fact, several patented PMH design/manufacturing technologies have already proven their ability to allow the automotive original equipment manufacturers (OEMs) and their suppliers to engage flexible assembly strategies, decrease capital expenditures and reduce labor required to manufacture a vehicle.

An example of a PMH automotive body-in-white (BIW) load-bearing component is depicted in Figures 1(a)–(b). The component in question is generally referred to as the "*rear longitudinal beam*" which connects, on the front end, to the rocker panel, in the middle to the shock tower, while at the rear end it connects to the rear cross beam. The traditional all-steel design of this component is displayed in Figure 1(a) and includes three sub-components: (a) main U-shape channel beam; (b) a reinforcement plate and (c) a cover plate. The latter two sub-components are spot welded to the first one. It should be noted that the cover plate is slightly shifted in Figure 1(a) in order to reveal the location of the reinforcing plate. The PMH rendition of the same component is depicted in Figure 1(b). The reinforcement plate has been replaced with an injection-molded thermoplastic cross-ribbed sub-structure, while the thickness of the cover-plate (not shown in Figure 1(b) for clarity) is reduced.

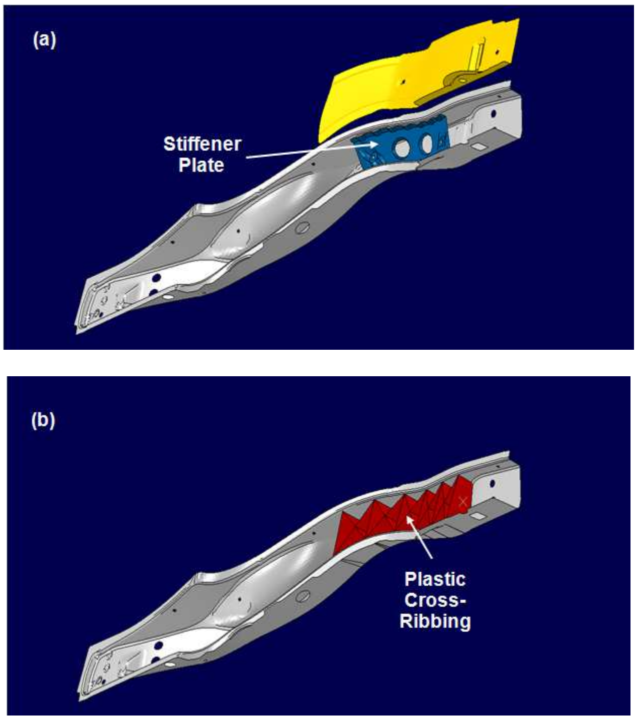


*Figure 1. An example of the: (a) All-metal and (b) Polymer Metal Hybrid (PMH) load-bearing automotive component.*

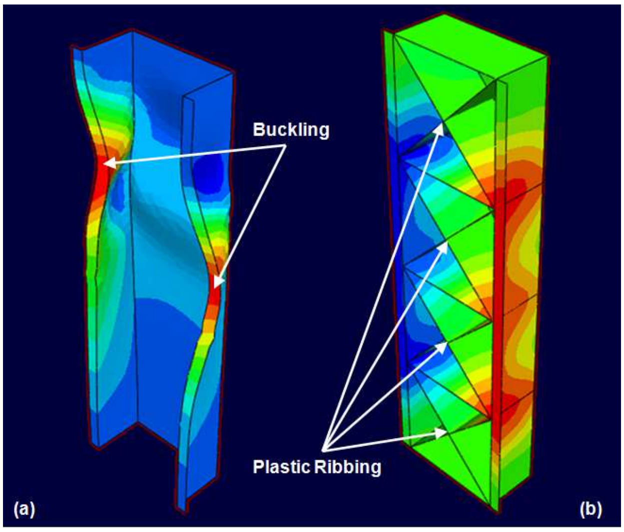


*Figure 2. The basic concept utilized in the PMH technologies. Buckling in an open-channel all-metal component in (a) has been prevented by a rib-like plastic substructure in (b) which provides the needed lateral support.*

The basic concept utilized in all PMH technologies is illustrated in Figures 2(a)–(b). An open-channel thin-wall sheet-metal component can readily buckle under compressive load, Figure 2(a). With very little lateral support, provided by a thin-wall cross-ribbed injection-molded plastic subcomponent, Figure 2(b), the buckling resistance (and the stiffness) of the component can be greatly increased (while the accompanying weight increase is relatively small).

Among many technical and economic benefits associated with the use of the PMH technologies, the following appear to be the most important: (a) reduction of the number of components; (b) production of the integrated components ready to assemble; (c) weight reduction compared to the traditional all-metal solutions; (d) additional design and styling freedom; (e) production of in-mold features like brackets, bosses and attachment points; (f) safety improvement due to lowered center of gravity of the vehicle; (g) a major (several-fold) increase in the bending strength of stamped metal sections. This effect is well understood and is attributed to the plastic subcomponent which forces the metal to maintain its cross-section properties throughout the loading cycle and delays the onset of failure due to localized buckling; and (h) improved damping in the acoustic range (relative to their all-steel counterparts, often as high as four times lower initial decibel reading measured in a simple hammer-strike test).

The first publicly-reported case of the introduction of the PMH technology into the automotive manufacturing practice is the PMH front end of the Audi A6 [11]. This component was produced by Ecia, Audincourt/France by injection over-molding a sheet-metal stamping with a cross-rib-shaped structure made of elastomer-modified polyamide PA6 - GF30 (type: Durethan BKV 130 from Bayer). Through direct mechanical testing of the PMH front end, it was demonstrated that the two constituent materials (i.e. metal and plastics) act synergistically to impart the mechanical performance to the PMH component which is not found in either of the two materials, *per se*.

Over the last few years, there has been an accelerated trend to replace all-steel structures in automotive front-end modules with their PMH counterparts. Besides their use in automotive front-end applications, PMH structures are finding an increased use in other automotive (e.g. instrument-panel and bumper cross-beams, door modules, tailgates, etc.) and non-automotive (e.g. appliance housings, bicycle frames, etc.) applications. In addition to an increased use of the PMH structures in automotive and non-automotive applications, new PMH technologies are being developed as alternatives to the classical over-molding method first established by Bayer/Ecia [11, 12].

## 2. Classification of PMH Technologies

Examination of all PMH technologies currently being employed in the automotive and non-automotive industries suggests that four major categories can be defined: (a) Injection over-molding technologies; (b) Metal over-molding technologies combined with secondary joining operations; (c) PMH technologies involving adhesive bonding; and (d) Direct-adhesion PMH technologies. Each of these categories of PMH technologies is briefly described below.

### 2.1. Injection Over-Molding PMH Technology

This process was originally introduced and patented by Bayer [12]. The process involves the following steps: (a) sheet-metal blanks are stamped to obtain desired (typically, U) shape of the metal inserts; (b) flared through-holes are punched into the metal inserts; (c) inserts are next placed in the injection-molding die; and (d) injection molding is used to over-mold the metal inserts with a cross-ribbed integrated structure made of 30% short glass-fiber-filled polyamide (i.e. nylon-6). In this process, tight interlocking between the metal insert and the short-fiber-filled nylon cross-ribbed structure, and the attainment of a superior combination of the PMH component stiffness and buckling resistance, are achieved through: (a) formation of rivets from the molten nylon which penetrated the insert through-holes; and (b) over-molding of the U-shaped insert flanges. A solid model of the simplified PMH component (consisting of an over-molded cross-ribbed nylon structure and a U-shaped metal stamping) produced by injection over-molding is displayed in Figure 3.

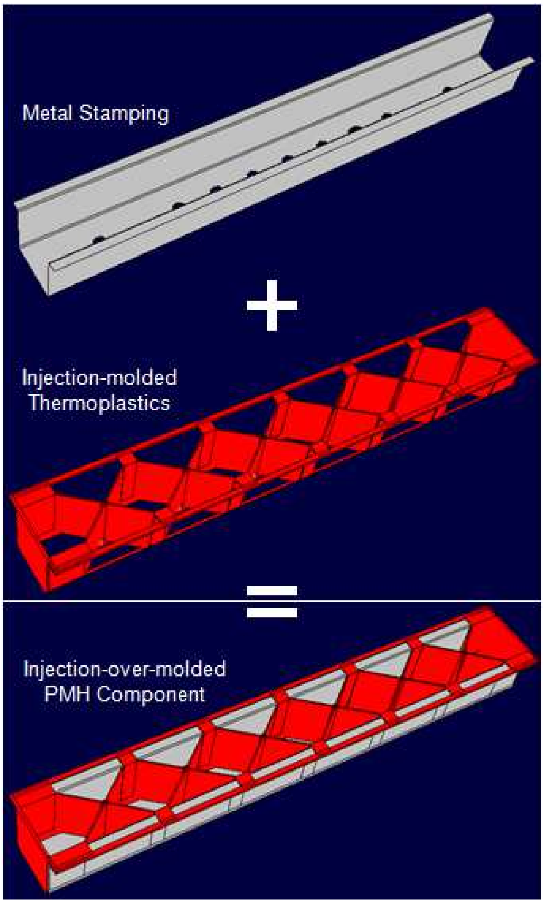


***Figure 3.*** *Exploded and integrated views of a prototypical injection-over-molded (simplified) load-bearing automotive body-in-white (BIW) PMH component.*

In the earlier renditions of this PMH technology, the over-molded cross-ribbed structure was limited to (extruded) two-dimensional geometries, due to the fact that an injection molding press normally opens in only one direction. In more recent renditions of this PMH technology, side motion of the tooling has been added, which enabled fabrication of multi-directional ribbed structures. These modifications in the cross-ribbed reinforcing nylon structure were found to yield significant improvements in the load-bearing capability of the PMH component relative to its U-shaped steel-stamping counterpart.

### 2.2. Metal Over-Molding PMH Technology

This PMH technology was originally developed and patented by Rhodia [13] and employed for the front-end module of a 2004 light truck intended for the South American market. The manufacturing process involves the following main steps: (a) a U-shaped steel stamping is placed in an injection mold and the underside of the stamping coated with a thin layer of short-fiber-filled nylon; (b) a separate injection-molding operation is used to fabricate a cross-ribbed nylon structure; and (c) lastly, in a secondary operation, the over-coated metal stamping and the cross-ribbed nylon structure are joined using ultrasonic welding. The main benefits of this PMH technology are: (a) potential for the fabrication of closed-section PMH components which, due to the continuous nature of the metal/polymer bond lines, exhibit a high load-bearing capability; and (b) enabling of functional integration like cable housings and air or water channels due to the hollow core of the PMH structure. In a more recent rendition of this PMH technology, gas or water injection-molding is employed in order to produce a stiffer, thinner coating for enhanced load-bearing capabilities and increased functional integration.

Another, low-cost rendition of this technology is the so-called Plastic-Metal Assembling process, also developed and patented by Rhodia [14]. The process comprises three main steps: (a) within the first step, a U-shaped steel stamping with punched holes and a nylon injection-molded component, which contains columns or heat stakes that can lock into the stamping holes, are produced separately; (b) next, the two sub-components are brought into contact while ensuring that the nylon columns penetrate the stamped holes; and (c) lastly, the two sub-components are joined using ultrasonic welding or heat staking to form locking rivets from the ends of the plastic columns.

### 2.3. Adhesively-Bonded Polymer-Metal-Hybrid Structures

This type of PMH technology was developed and patented by Dow Automotive [15], and introduced in 2003 in prototype form for a Volkswagen front-end module. This process involves three main steps: (a) a separate fabrication of the metal stamping and the injection-molded cross-ribbed structure made of short-glass-fiber filled poly-propylene; (b) application of Dow's proprietary low-energy surface adhesive (LESA) to the sub-components to be joined using high-speed robots; and (c) curing of the resulting adhesive joint. Often, to help maintain alignment of the sub-components during curing of the adhesive, snap features are designed into the sub-components.

The main additional advantages of this PMH technology are: (a) the acrylic-epoxy adhesive LESA does not require cleaning or other types of pre-treating of the low surface-energy poly-propylene; (b) adhesive bonding creates continuous bond lines, minimizes stress concentrations and acts as a mechanical buffer which absorbs and delocalizes contact stresses between the metal and polymer sub-components; (c) adhesively-bonded PMHs enable the creation of closed-section structures which offer high load-bearing capabilities and the possibility for enhanced functionality (e.g. direct mounting of air bags in instrument-panel beams or incorporation of air or water circulation inside door modules); and (d) through proper selection of the LESA grade, adhesively-bonded PMH structures can be optimized with respect to their stiffness, buckling resistance, toughness, adhesion strength and cure time.

### 2.4. Direct-Adhesion Polymer-Metal-Hybrid Technology

This PMH technology is currently being developed [16–17] and is aimed at addressing some of the main limitations of the aforementioned three PMH technologies. Among a number of limitations/shortcomings of the current PMH technologies, the following appear to be most noteworthy: (a) the injection over-molding process requires the presence of through-holes in the metal stamping for the formation of the interlocking rivets. However, the presence of these holes may compromise the functionality and/or mechanical performance (or even structural integrity of the critical load-bearing) PMH components; (b) the injection over-molding process also requires over-molding of the metal-stamping flanges for effective metal-to-polymer interlocking. Since these flanges are often needed for spot welding purposes, their over-molding may not be allowed; and (c) in the case of adhesively-bonded PMH structures, the high cost of the adhesive, the relatively long curing time and the limited ability of the adhesive to withstand aggressive chemical and thermal environments encountered in the paint-shop during body-in-white (BIW) pre-treatment and E-coat curing may be considered as potential limitations.

Within the direct-adhesion PMH technology, the joining between the metal and thermoplastic sub-components is attained through direct-adhesion of injection-molded thermoplastic cross-ribbed structure to the metal without the use of interlocking rivets, over-molded edges or structural adhesives [18]. Within this PMH technology, various mechanical, physical and chemical phenomena and processes are taken advantage of in order to attain a desired level of polymer-to-metal adhesion strength. As reported in Ref. [19], polymer-to-metal direct-adhesion technologies can be classified as:

(a) Technologies relying on surface roughness length-scale polymer/metal mechanical interlocking phenomena [e.g. 20–22]. While still of a mechanical interlocking character, the mechanism of plastic-to-metal joining in the case of these PMH direct-adhesion technologies is distinct from that found in the standard *insert over-molding* process which relies on the shrink-fit phenomenon and special under-cut geometrical features for good polymer-to-metal load transfer. In the case of direct-adhesion PMH technologies relying on polymer/metal mechanical interlocking phenomena, polymer/metal interlocking occurs by the infiltration of the micron-size roughness features of the metal substrate by the molten plastic and, upon solidification, the formation of mechanical micron-size interlocks. It is well-established [20–22] that for successful polymer/metal joining, metal subcomponent preheating is extremely critical. It was suggested in [19] that metal subcomponent preheating can be effectively achieved by integration of an induction heater into the injection-molding mold;

(b) Technologies employing in-coil or stamped-part metal priming with adhesion promoters [e.g. 23, 24]. The most frequently used primer is silane which, owing to its amino and vinyl functional groups, acts as a *"coupling agent"* which promotes adhesion between inorganic (metallic, in the present case) and organic (polymeric, in the present case) materials. For silane to act as an adhesion promoter, its organo-reactive moieties must be in contact with polymer and metal which is achieved by coating the metal substrate with silane just prior to injection molding of the polymer [25]. It is generally believed that the silane coupling reactions take place in the following sequence: (i) hydrolysis of the alkoxy group which results in the production of hydrogen; (ii) formation of the hydrogen bonds at the polymer/metal interface; (iii) interfacial condensation of the functional groups; and lastly (iv) interfacial chemical reactions with the polymer and metal resulting in the formation of interfacial bonds [26];

(c) Technologies based on chemical modifications of the injection-molding thermoplastic material for enhanced adhesion to metal [e.g. 27, 28]. Efforts have been reported in the open literature involving modification of either polymerized thermoplastic material (through the formation of polymer blends, [27]) or at the monomer level (through direct changes in the monomer chemistry). In the work reported in Ref. [10], poly-amide was chemically modified by blending it with self-ordering poly-(ester-amide) block co-polymer (a hot-melt adhesive-like material). The resulting polymer blend was found to exhibit an exceptionally high adhesion strength (>20MPa) even in the cases in which metal surfaces were not pre-cleaned and were left covered with drawing compound/oil prior to injection over-molding.

An example of chemical modification of the thermoplastic resin for enhanced polymer/metal adhesion, was reported in Ref. [28]. In this work, the effect of direct addition of various concentrations of styryl silane to styrene (monomer) resin on the ability of the resin to directly bond to aluminum upon polymerization was investigated. It was found that the concentration of styryl silane in styrene resin affected: (i) the thickness of the polymer-to-metal bonding interface; (ii) the polymer/metal adhesion strength; and (iii) the bond-strength sensitivity to the presence of moisture. In addition, the results revealed that metal-surface preparation via either chromic-sulfuric acid etching or phosphoric acid anodization is highly critical for attaining good polymer-to-metal adhesion. This observation was rationalized by the role of etching surface treatment in ensuring that a sufficient density of binding sites is available to provide grafting or tethering of the polymer interfacial layer to the metal surface.

The thickness of the interfacial layer, which is controlled by the concentration of silane in the styrene monomers, has been found to have a dominant effect on the adhesion strength. Specifically, when the thickness of the polymer interfacial layer becomes comparable with the average distance between the polymer-chain entanglement points, the polymer-to-metal adhesion strength attains its maximum value;

(d) So-called “*clinch-lock*” PMH technology [8] which utilizes some ideas from the spot-clinching sheet-metal mechanical fastening/joining process. Specifically, stamping is used to produce shallow millimeter-size *“dove tail”* shape impressions/ indentations into the metal subcomponent/stamping. These impressions ensure that the subsequently injection over-molded thermo-plastic subcomponent is securely anchored to the metal subcomponent. The joint provides effective metal/polymer connectivity by at least two distinct mechanisms: (i) mechanical interlocking; and (ii) enhanced adhesion due to an increased metal/polymer contact surface area; and

(e) Other approaches aimed at enhancing polymer-to-metal direct-adhesion through physical and chemical modifications in the metal-subcomponent surface [29–32]. For example, in Ref. [31], Openair® plasma is utilized to modify metal subcomponent surface via the combination of the following mechanisms: (i) surface cleaning, e.g. the removal of organic contaminants; (ii) ablation, which removes weakly-bonded surface layer; and (iii) potential chemical modification due to enhanced surface reactivity and the potential for the occurrence of surface chemical reactions.

# 3. Mechanisms for Polymer/Metal Joining

It is well-established [e.g. 1] that structural/functional performance of a PMH component depends greatly on the extent of load transfer through the polymer/metal interfaces which, in turn, is controlled by the mechanism and strength of polymer-to-metal joining. Hence, it is important to identify and understand the nature of this joining across the four aforementioned groups of PMH technologies.

## 3.1. Injection Over-Molded PMH Structures

In this case, polymer-to-metal load transfer is carried out through purely mechanical component-length-scale polymer/metal joints. These joints rely on the operation of shrink-fit phenomena and on the formation of mechanical interlocks promoted by the presence of special under-cut geometrical features within the metal subcomponent.

## 3.2. Metal Over-Molded PMH Structures

In this case, it is the interface between the coating and the metallic subcomponent that plays a critical role in the load transfer, since the interface between the injection-molded polymeric subcomponent and the coating, after ultrasonic welding, is effectively seamless. As will be discussed below, in conjunction with the direct-adhesion PMH technologies, there are a number of potential (mechanical and chemical) polymer/metal adhesion mechanisms.

## 3.3. Adhesively-Bonded PMH Structures

In this case, polymer-to-metal interface is replaced with a thin-layer structural interphase. Due to the presence of a large number density of interfacial covalent bonds, the interphase layer is typically stiff and strong and enables almost complete load transfer between the two PMH components.

## 3.4. Direct-Adhesion PMH Structures

As reviewed earlier, there are several direct-adhesion PMH technologies and they rely on different polymer/metal joining mechanisms. For example, one class of direct-adhesion PMH technologies relies on the formation of surface roughness length-scale polymer/metal mechanical interlocks [e.g. 20–22] which are formed as a result of the infiltration of the surface roughness features of the metal substrate by, and subsequent solidification of, the molten plastic. On the other hand, in the case of the direct-adhesion PMH technology which employs metal surface priming, as in the case of cold-rolled mild steel stamping primed with amino-silane and over-molded with poly-(vinyl chloride), PVC [23], the polymer/metal joining mechanism is rationalized as follows: (a) amine hydrochloride complexes appear to form by protonation of amino groups of the silanes with HCl that was liberated from PVC during the onset of thermal dehydro-chlorination; (b) furthermore, quaternization or nucleophilic substitution of labile pendent allylic chloride groups by amino groups on the silanes takes place, thus grafting PVC onto the amino-silanes. It was determined that PVC having β-chloroallyl groupings along its chains showed better adhesion with steel pre-coated with amino-silanes; and (c) interdiffusion of the polymer phase and the silane phase was found to be also critical in obtaining good adhesion.

## 4. Results

In order to assess the potential of PMH technologies for use in load-bearing automotive body-in-white (BIW) structural components, various multi-disciplinary computational methods and tools have been utilized by a number of researchers, designers and manufacturing engineers (e.g. [18, 33]). The analyses cover the following aspects of the PMH component design, fabrication, performance and end-of-life considerations:

(a) application of the engineering design optimization methods and tools to the design of an automotive BIW PMH component which meets functional requirements (e.g. those related to stiffness, strength and buckling resistance) while accounting for the component manufacturability constraints;

(b) detailed computational fluid dynamics numerical simulation of the filling (including flow-induced changes in fiber orientation), packing, and cooling stages of the injection molding process used to fabricate PMH short-fiber-filled polymeric subcomponent, and an anisotropic thermo-visco-elastic computation of the thermally- and pressure-induced (in-mold) stresses in an injection-molded short-fiber-filled polymeric subcomponent;

(c) structural mechanics analysis (based on the use of multi-layer shell elements) of shrinkage and warping caused by the relaxation of the in-mold stresses after polymeric-subcomponent (in the case of metal over-molding or adhesive-bonding-based PMH technologies) or hybridized subcomponent (in the case of injection over-molding and direct-adhesion-based technologies) ejection from the injection-molding mold; and

(d) structural mechanics analysis (including the effect of adhesion-based load transfer between metallic and polymeric subcomponents) of the PMH component stiffness and strength under several simple monotonic loading modes and under creep.

In the remainder of this section, a brief overview is provided of these computational analyses.

### 4.1. PMH Component Design and Optimization

Due to ever-more restrictive lightweight targets and the demands for shortened product development time-scale in the automotive industry, a continuous need has arisen for an integration of advanced computer aided optimization methods into the overall component/sub-assembly design process. This is particularly true in the case of structural load-bearing PMH BIW automotive components. In most cases, the design of the load-bearing PMH components is driven not only by stiffness and buckling-resistance requirements but also by strength requirements (e.g. to obtain the required performance in side-impact collisions).

Automotive BIW structural PMH components are typically designed using the following finite-element based two-step engineering design-optimization procedure: (a) topology optimization is performed first to obtain a general idea about an optimal configuration of the BIW component in question which ensures mass-efficient load paths; and (b) the component topology obtained in (a) is next interpreted to form an engineering design which is then optimized under real functional requirements, using non-linear finite-element based, detailed size- and shape-optimization methods and tools. Within these optimization procedures, geometrical and material aspects of the PMH component are treated as design variables, the objective functions are defined in terms of the functional performance requirements (as typically quantified by the required levels of stiffness, strength or buckling resistance) while constraints are generally associated with component manufacturability, material compatibility with the BIW manufacturing process chain, cost, etc. Examples of the results obtained using strength-based topology and detailed-design optimization procedures for a simplified automotive BIW structural PMH component are shown in Figures 4(a)–(b), respectively.

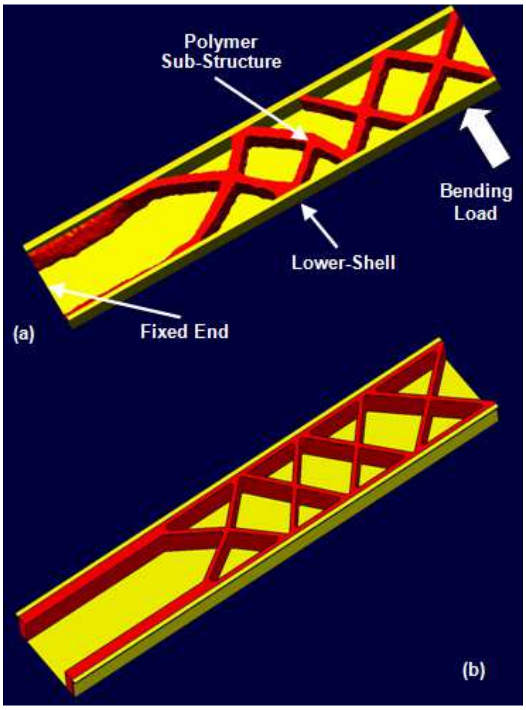


*Figure 4. Results of strength-based: (a) topology; and (b) detailed-design optimization procedures for a simplified automotive BIW structural PMH component.*

### 4.2. Modeling and Simulations of the Injection-Molding Process

Thermoplastics injection molding is a widely used manufacturing process for producing parts/components with a high degree of geometrical complexity. A typical injection molding process involves four distinct stages: (a) *filling* of the mold with molten thermoplastics; (b) *packing* – injection of additional material into the mold under high pressure to compensate for the cooling-induced volumetric shrinkage of the material; (c) *cooling* which gives rise to the solidification of the material residing in the mold; and (d) *ejection* of the solidified part/component from the mold. During the filling, packing and cooling stages of the injection molding process, the material is subjected to complex thermo-mechanical loading which gives rise to the changes in local specific volume (density), component shape as well as to the development of the in-mold stresses within the component. In other words, while the (thin-wall) component resides in the mold, it is constrained by the mold causing internal stresses to develop within the component during solidification of the melt and subsequent cooling. Upon ejection, these stresses relax causing distortion/warping and further shrinkage of the molded component. Further warping and shrinkage of the component may occur during cooling to room temperature of the ejected molded component.

To take into account the fact that the injection-molded plastic subcomponent is made of short-fiber-filled thermo-plastics, and hence, may possess a heterogeneous, non-isotropic material, the following injection-molding process simulation sub-analyses are generally carried out: (a) identification of the optimal placement and the number of thermoplastic-melt injection points; (b) mold-filling; (c) melt-flow-induced changes in the fiber orientation distribution; (d) mold-packing; and (e) in-mold stresses. These sub-analyses are briefly reviewed below.

*Optimal Placement and Number of Injection Points:* Before simulations of the injection molding process can be carried out, the optimal placement and the number of injection points (gates) has to be determined. To determine an optimum number and location of the gates, a constrained optimization analysis is typically employed within which optimum values of the objective function (the degree of balanced flow which ensures that regions within the mold which are furthest away from the gate(s) are filled at approximately the same time [34]) is attained through the selection of the number and location of injection-points (design variables) while meeting the constraints imposed by: (i) the component geometry; (ii) the properties of the thermoplastic melt; (iii) the specified injection-molding process parameters; and (iv) injection-molding feasibility (i.e. successful filling of the sections associated with the minimum plastics-wall-thickness).

*Mold-Filling Analysis:* Earlier computational efforts reported in the literature were mainly focused on predicting pressure and temperature distributions within the mold cavity and melt-front advancement during mold filling [35–40]. More recent computational efforts, on the other hand, have also addressed post-filling phenomena such as flow-induced changes in the fiber orientation distribution, and the development of in-mold stresses within the component [41, 42]. Furthermore, while the early efforts employed mainly empirical material and melt/mold interaction models [e.g. 42], the more recent computational investigations employed more physically-based material models and contact algorithms [e.g. 43].

Within the mold-filling analysis, the three basic conservation equations, i.e. the mass, momentum and energy conservation equations, are integrated spatially and temporally using a (typically explicit) numerical scheme. In the case of semi-crystalline polymeric materials, the aforementioned partial differential equations have to be combined with an additional (differential or algebraic) equation defining the rate of crystallization.

It should be noted that, when a mold-filling computational analysis involves short-fiber-filled thermo-plastics, the melt-flow local field is generally assumed to be independent of the orientation distribution of the fibers. On the other hand, the flow field causes re-orientation of the fibers and changes in their local orientation distribution. Strictly speaking, the exclusion of the effect of fiber orientation on the local flow field is justified only in the case of injection molding of the thin-walled components, in which the fibers are oriented nearly parallel to the plastic-wall mid-plane and, hence, their interaction with the melt flow is limited [44–49]. The conditions which have to be satisfied in order for the influence of the fiber distribution function on the flow to be neglected can be found in Ref. [50].

Since injection molding of PMH subcomponents or over-molding of the PMH components involves melt flow through thin mold-cavity channels, through-the-thickness-variations in pressure are generally neglected and the melt flow is treated to be of a Hele-Shaw flow character [51]. Consequently, mold-filling analysis is simplified and involves not the direct solution of the governing conservation equations but rather a solution of the pressure-based (elliptical partial differential) Hele-Shaw flow equation [51]. When solving the Hele-Shaw flow equation, the shear-rate, pressure and temperature dependencies of the material viscosity must be specified. This is typically done using the Cross model [43]. Furthermore, the following boundary conditions are typically used in conjunction with the Hele-Shaw equation: (a) Either the inlet-flow rate or the pressure boundary condition are defined at the injection points; (b) A zero-pressure condition is defined on the advancing flow front; and (c) A zero-normal-pressure gradient is specified over the mold-cavity-surface. While these boundary conditions do not generally ensure a *"no-slip"* condition over the mold-cavity-surface (and may allow the fluid to *"slip"*), the resulting inaccuracies in the velocity-field predictions are typically found not to be significant [52].

Since the Hele-Shaw flow equation considers only the flow parallel with the local mid-plane, it does not account for the fountain flow and may lead to inaccuracies in the temperature and fiber-orientation predictions. These inaccuracies are generally mitigated using one of the local approximations [39].

One of the results of the mold-filling analysis is determination of the instantaneous location of the flow front. Typically, the flow front is tracked by discretizing the mold cavity into a large number of control volumes and by determining the state of filling of each control volume.

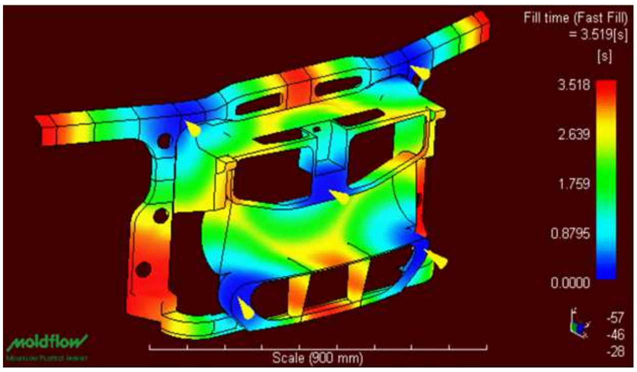


***Figure 5.*** *An example of the mold-filling analysis results showing spatial distribution of the local filling time for the case of a vehicle PMH front-end module. (Please note that metallic stampings are not visible since they are placed within the mold cavity.)*

An example of the mold-filling analysis results showing spatial distribution of the local filling time for the case of a vehicle PMH front end module is shown in Figure 5. (Five injection ports are marked as yellow cones.) It should be noted that metallic stampings are not visible since they are placed within the mold cavity.

Another result of mold-filling analysis is the temporal evolution of the temperature field. This result is obtained by solving numerically the energy conservation equation in which the heat convection and viscous dissipation terms from a previous time step are treated as source terms during the current time step. Furthermore, to account for high rate of heat conduction through the metal subcomponent (in the case of injection over-molding and direct-adhesion PMH technologies) or over the injection mold internal surfaces (in the case of metal over-molding and adhesion-bonding PMH technologies), time-dependent, uniform temperature-based boundary conditions (determined using a separate boundary element analysis [53]) are employed. It should be noted that the use of this boundary condition assumes temperature continuity at the polymer/metal and polymer/mold interfaces. In other words, the effect of interfacial heat conductance is neglected.

*Flow-Induced Fiber Orientation Distribution Analysis:* As mentioned above, melt flow through the mold cavity causes re-orientation of the fibers and changes in their local orientation distribution. For accurate predictions of the shrinkage and warping of an injection-molded component made of short-fiber-filled thermo-plastics, knowledge of the flow-induced fiber-orientation distribution throughout the component is critical [e.g. 54–56]. Since most commercial short-fiber-filled thermo-plastics commonly used for injection molding can be characterized as semi- or highly-concentrated suspensions, fiber/fiber interactions and the associated spatial constraints to the fiber motion may significantly affect the final fiber-orientation distribution in the injection-molded component. Typically, fiber/fiber interactions are accounted for in computational analysis of the injection molding process through the use of the Folgar-Tucker model [54]. In this model, an isotropic symmetric second-order fiber/fiber interaction tensor is introduced in the diffusion term of the equation of motion for an isolated fiber in a Newtonian fluid [57]. The components of this interaction tensor, as a function of the initial fiber orientation distribution, fiber aspect ratio, the number density of fibers in the suspension, the melt properties, and the shear-strain magnitude, are assessed using direct numerical simulations of fiber/fiber interactions within simple-shear flow [55]. In these simulations, short-range interactions are quantified using a lubrication model [58] while long-range interactions are calculated using a boundary element method [58].

Once the components of the interaction tensor are determined for a given short-glass-filled thermoplastic polymer melt, they are used, throughout the mold cavity, within an anisotropic rotary diffusion equation to define local rate of change of the fiber orientation distribution function as quantified by the second-order fiber-orientation distribution tensor. Time-integration of this rate of change gives temporal evolution of the fiber orientation distribution function during mold-filling.

*Mold-packing Analysis:* As mentioned earlier, mold-packing involves injection of additional melt into the mold under high pressure to compensate for the cooling- and solidification-induced volumetric shrinkage of the material. While the packing phase of the injection molding process is governed by the same conservation equations as the filling phase, an additional equation, the equation of state, must be defined in order to include the effect of melt compressibility. The equation of state typically used in mold-packing analysis defines a functional relationship between the pressure, specific volume, temperature, and cooling rate.

It should be noted that the presence of the cooling rate term in the equation of state enables modeling of various phase transformations (such as freezing, crystallization, and ductile-to-glass transition) accompanying the packing process. Furthermore, it should be noted that various material properties such as volumetric thermal expansion coefficients and compressibility, and their temperature and pressure dependencies, are derived from the equation of state.

*In-mold Stress Analysis:* There are two main sources for in-mold stresses in injection-molded components: (a) Visco-elastic deformations of the thermoplastic material during filling/packing can give rise to the development of the so-called "*flow-induced*" in-mold stresses; and (b) Restrictions to the (often inhomogeneous) cooling- and solidification-induced shrinkage of the polymer due to the mold walls and the applied packing pressure may lead to the generation of the so-called "*thermally- and pressure-induced*" in-mold stresses. It is generally assumed that the flow-induced in-mold stresses are relatively small and that they are readily relieved while the component resides in the mold at high temperatures prior to ejection. Consequently, they are typically neglected in an in-mold stress analysis. As far as the thermally- and pressure-induced in-mold stresses are concerned, they have been extensively investigated computationally [e.g. 59–68]. These investigations clearly revealed the effects of mold-wall constraints and thermo-plastic material properties on the extent and distribution of the in-mold stresses.

Computation of the in-mold stresses entails the knowledge of high-fidelity material models (in particular, the time-dependent portion of the material model). This is related to the fact that as the injection-molded component begins to cool inside the mold, the relaxation time of the thermo-plastic material starts to increase and to approach the in-mold component resident time. Due to the small magnitude of the attendant in-mold strains, the thermo-plastic material behavior can be satisfactorily represented using an anisotropic linear thermo-visco-elastic material model [e.g. 69, 70]. Typically, within such models, the viscous portion of the material response assumes interchangeability between the time and temperature effects. In other words, materials are assumed to be *thermo-rheologically simple*. It should be noted that this assumption may not be fully justified in the case of short-fiber-filled polymers used in PMH structures. For amorphous polymers, this time/temperature interchangeability is generally represented using the WLF equation [71]. On the other hand, for semi-crystalline materials, this interchangeability is based on an Arrhenius-type expression [e.g. 1].

As established above, since the thermo-plastic material used in PMH components is typically filled with short fibers and the flow causes the orientation distribution function to deviate from a random one, the material locally behaves anisotropically. To quantify anisotropic aspects of the material behavior from the knowledge of the polymeric melt and fiber properties as well as from the knowledge of the fiber orientation distribution function, one typically employs one of the micro-mechanics based homogenization procedures. A brief discussion of these procedures is presented in the next section.

Once the appropriate material model has been constructed, temporal evolution of the in-mold stresses can be determined by carrying out a time-dependent thermo-/visco-elastic structural analysis. Within this analysis, the temperature field is imported from the filling and packing analyses.

To simplify in-mold stress analysis, the following assumptions/simplifications are typically used: (a) through-the-wall-thickness normal stress is locally constant in the through-the-thickness direction; (b) as long as through-the-wall-thickness normal stress is compressive, the injected polymer is considered to be in contact with the metal subcomponent/mold; (c) locally, a component is fully constrained within the mid-plane and, hence, the only nonzero strain component is the one in the through-the-thickness direction; and (d) metallic subcomponent/mold are assumed to be rigid.

The in-mold stress analysis is typically carried out under the following stress-based boundary conditions:

(a) When the component resides in the mold and the injected material contains both a solid outer-layer and a liquid core, the through-the-thickness normal stress is set equal to the negative fluid pressure; or

(b) When the component resides in the mold and the injected material has completely solidified, the component may either be in contact with the metal subcomponent/mold or be separated from it. In the first case, the through-the-thickness normal stress is determined using the condition that the average through-the-thickness normal strain is zero. In the latter case, the through-the-thickness normal stress is set to zero.

*Micro-Mechanics-based Derivation of the Effective Material Properties:* As established earlier, glass-filled polymeric materials used in PMH components become anisotropic during mold-filling due to flow-induced changes in the (initially random) orientation distribution of the fibers. Typically, micromechanics-based homogenization models are utilized to derive (anisotropic) elastic and thermo-elastic properties of fiber-filled thermo-plastic materials used in PMH technologies from the knowledge of the properties of the constituent fiber and matrix materials and the known fiber-orientation distribution function [72]. It is generally assumed that the injection-molded material is transversely isotropic, i.e. its properties are equal in the transverse and the through-the-thickness directions. Consequently, the elastic response of such materials is defined by five (temperature-dependent) elastic moduli while the thermo-elastic response is defined in terms of two (longitudinal and transverse) linear coefficients of thermal expansion.

The (homogenized and isotropic) elastic and thermo-elastic properties of fiber-filled thermoplastics are typically assessed using the following two-step micro-mechanics procedure: (a) first, the properties of a material, in which the fibers are perfectly aligned, are assessed using a homogenization scheme within which the material at hand is considered as an aggregate of discrete constituent materials [e.g. 72, 73]; and (b) next, an orientation averaging procedure is applied to include the effect of the attendant fiber-orientation distribution on the effective elastic and thermo-elastic material properties [e.g. 74].

### 4.3. Ejected-Component Shrinkage and Warping Analysis

While the injection-molded material resides in the mold, it is constrained and cannot distort. However, after ejection, the component can undergo shrinkage and warping. On the other hand, in the case of an ejected PMH component, the thermo-plastics subcomponent remains somewhat constrained by its adhesion to the steel subcomponent/stamping.

The same thermo-visco-elastic structural mechanics analysis used to determine in-mold stresses is often employed in order to analyze shrinkage and warping of a polymeric-subcomponent (in the case of metal over-molding or adhesive-bonding-based PMH technologies) or hybridized subcomponent (in the case of injection over-molding and direct-adhesion-based technologies) after ejection from the injection-molding mold. Since the shrinkage/warping analysis is generally not carried out within the mold-filling analysis but rather within a separate structural mechanics finite-element program, the spatial (including through-the-thickness) variations in thermo-mechanical material properties (a material-model definition) and the in-mold stresses (initial conditions) have to be imported from the injection molding process analysis (where they were originally computed). After the part is ejected from the mold, no external loads are applied to it and, hence, the following boundary conditions are employed: (a) six (three translational and three rotational) degrees of freedom of one of the ejected component material points are constrained in order to prevent uncontrolled rigid body motion of the component; and (b) zero-traction boundary conditions are applied over the ejected-component surfaces.

### 4.4. PMH Component Structural Analysis

The ejected (warped) PMH component, after cooling to room temperature, is subjected to a series of structural (quasi-static and dynamic) finite-element analyses in order to validate its functionality and assess its mass efficiency. This is typically done by comparing the performance of the PMH component against the performance of the corresponding all-metal component, the PMH component is intended to replace. An example of the results obtained in such analyses involving an idealized load-bearing BIW component [10] is displayed in Figures 6(a)–(f).

The all-metal rendition of this component (used as a control) consists of a flanged U-shaped stamping and a cover plate (spot-welded) along the length of the flanges, Figure 6(a). Within the finite-element analysis employed, each spot weld is modeled as a kinematic constraint distributed over a circular region (corresponding to the spot-weld size) of the contacting surfaces. The resultant closed-box configuration generally provides a good combination of compressive, bending and torsional stiffnesses and strengths but, in the case of the all-steel construction, the weight of the component is relatively high.

To form a PMH rendition of the simplified load-bearing BIW component, the all-metal control is modified in the following way: (a) the cover plate is eliminated; and (b) a plastic insert consisting of an overlay (mates with the interior of the U-shape channel) and a series of *"cross"* ribs is added. To ensure that the plastic insert will not be affected by welding of the U-shape channel ends to the BIW structure, the length of the insert is set to 80% of the U-shape channel length and the insert is centered relative to the channel lengthwise. The resulting configuration of the PMH component is shown in Figure 6(b). Within the finite element analysis of the PMH component, adhesion between the metal and the polymer is simulated using specialized cohesive elements which, through the use of normal and tangential traction-separation relations, enable modeling of the initial loading, the initiation of interfacial damage, damage-induced adhesion stiffness/strength degradation and the propagation of damage leading to eventual decohesion of the adhering surfaces, e.g. [1].

To validate functional performance of the PMH component under quasi-static loading conditions, the control and the PMH component are each subjected to four basic loading modes: (a) longitudinal (i.e. $x$-axis) compression, Figure 6(c); (b) bending about the first transverse (i.e. $y$-axis) direction, Figure 6(d); (c) bending about the second transverse (i.e. $z$-axis) direction, Figure 6(e); and (d) twisting about the longitudinal (i.e. $x$-axis) direction, Figure 6(f). It should be noted that in Figures 6(c)–(f), the four deformation modes are displayed only for the PMH component, for brevity. Structural mass efficiency of the PMH component is assessed by comparing mass-normalized load and torque peak values between the control and the PMH component. An example of such a comparison is given in Figures 7(a)–(b). The results displayed in Figures 7(a)–(b) suggest that the PMH component outperforms its all-steel counterpart relative to $x$-compression and $z$-bending load-bearing resistances while the two are on par relative to their $y$-bending and $x$-torsion strengths.

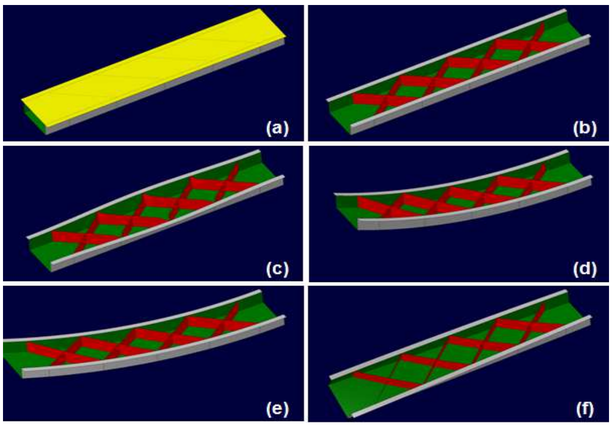


***Figure 6.*** *Structural analysis of the PMH component: (a) all-metal control; (b) PMH component; (c) axial compression; (d) bending about first transverse direction; (e) bending about second transverse direction; and (f) twisting about the longitudinal direction.*

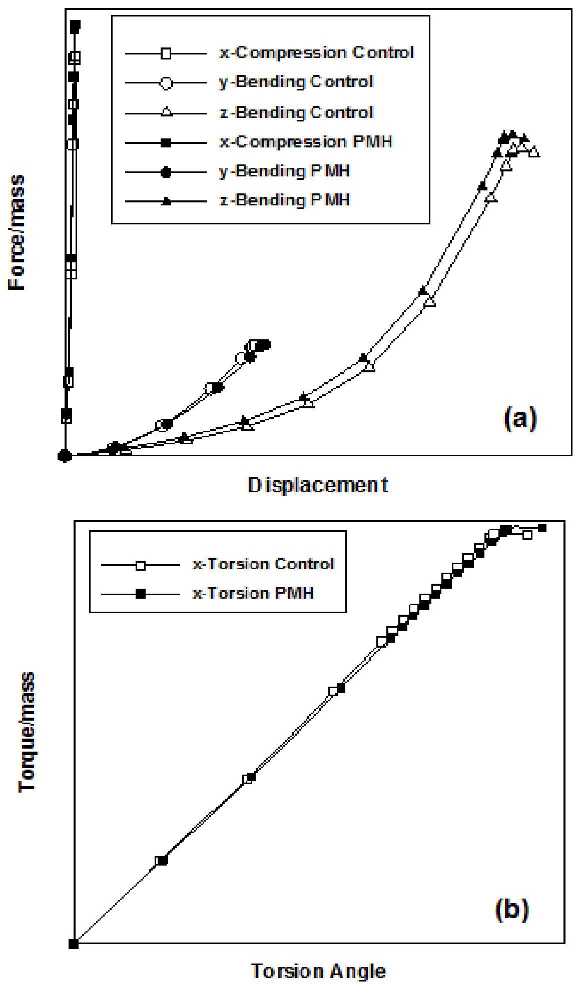


***Figure 7.*** *Typical results pertaining to: (a) mass-normalized force vs. displacement; and (b) mass-normalized torque vs. torsion angle for the all-steel (control sample) and PMH component (experimental sample) used for validation of the PMH-component functionality/utility.*

## 5. Discussion

When selecting among the previously overviewed PMH technologies for use in various automotive manufacturing applications, consideration is given to the total-life-cycle (*TLC*) of the PMH component in question as well as the TLC of the vehicle. The TLC PMH technology selection approach differs from the more conventional manufacturing-process selection approach [e.g. 7, 75, 76] which primarily emphasizes issues related to the component function and performance. The TLC approach, on the other hand, considers the potential consequences and ramifications associated with the PMH technology selection to various stages of the vehicle manufacturing process chain, vehicle performance and durability (while in service), as well as the analysis of various End-of-the-Life-of-the-Vehicle (*ELV*) issues (e.g. disassembly, suitability of the material(s) for shredding, and segregations, potential for economic recycling, etc.). A schematic of the major stages in the life of a BIW component for which the PMH technology is being selected (using the TLC approach) is depicted in Figure 8. When considering potential consequences of the PMH technology selection relative to the automotive BIW manufacturing process chain, one of the key issues is compatibility of the selected PMH technology with the main manufacturing-process steps which include: (a) metal-subcomponent manufacturing by stamping in the process shop; (b) PMH component or thermoplastic sub-component manufacturing in the injection-molding shop; (c) BIW construction by various joining processes in the body shop; and (d) BIW pre-treatment and painting in the paint shop. It should be noted that, as indicated in Figure 8, bolt-on (i.e. non-structural) and load-bearing (i.e. structural) BIW components have somewhat different manufacturing history. These differences are caused by the fact that, since structural components are integrated into the BIW frame in the body shop, they have to pass through (and be compatible with the requirements of) the paint shop. On the other hand, it is not necessary for bolt-on components to pass through the paint shop since they can be directly attached to the painted BIW frame in the assembly shop.

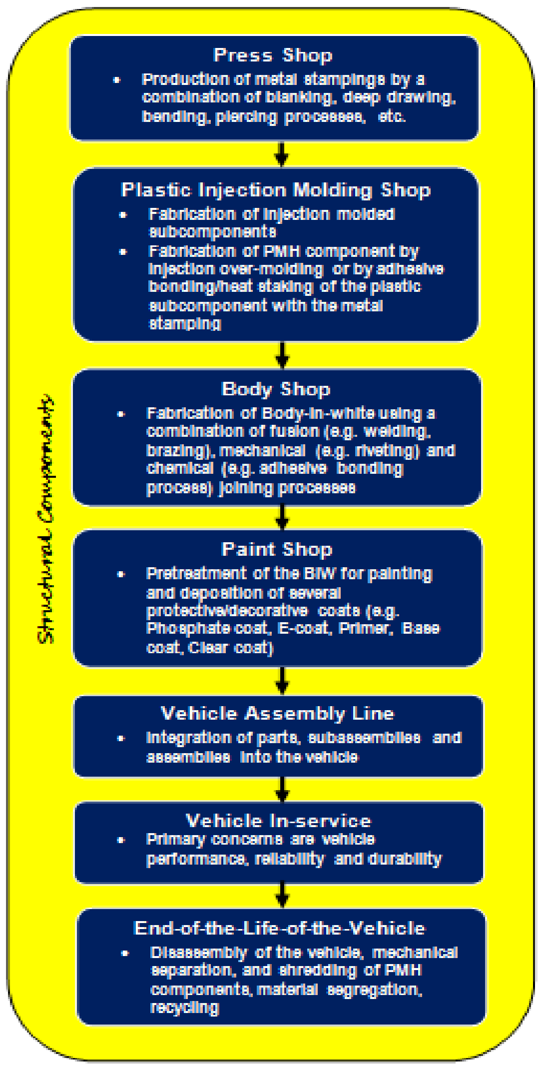


***Figure 8.*** *Key life-cycle stages for a typical PMH automotive BIW component.*

As an example of a BIW manufacturing process chain requirement for the PMH technology, one may take the case of selection of the material for the polymeric sub-component. In the body shop, the key functional requirement for the polymeric sub-component material is its ability to withstand welding-induced high-temperature exposures. On the other hand, the main functional requirements for the polymeric sub-component material relative to its compatibility with the BIW paint shop deal with the ability of the selected material to withstand mechanical, thermal and chemical attacks without degrading and without contaminating the paint baths.

## 6. Conclusions

In this chapter, a comprehensive overview has been provided of the key aspects of injection over-molding technologies used in automotive BIW structural applications. Specifically, the following aspects of injection-molding technologies have been discussed: (a) fundamental concepts related to synergistic polymer/metal interactions; (b) classification of the technologies; (c) basics of polymer/metal adhesion and load transfer; (d) application of computational engineering methods and tools for process and product-performance simulations; and (e) compatibility of different injection-molding PMH technologies with the automotive BIW manufacturing process chain. It has been argued that, while the utilization of the PMH technologies in the manufacture of automotive BIW may yield benefits related to lower vehicle weight, improved fuel economy and cost, vehicle end-of-life issues must be considered when selecting these technologies. Specifically, increasing emphasis on sustainability, dwindling material supplies, increasing producer responsibility, product take-back legislations, and marketing of recycled material-content claims, require consideration of the issues such as product refurbishment, product dis-assembly, materials extraction and procurement, and end-of-life product management.

## References


[1] Grujicic M, Sellappan V, Arakere G, Seyr N, Erdmann M. Computational Feasibility Analysis of Direct-Adhesion Polymer-To-Metal Hybrid Technology for Load-Bearing Body-In-White Structural Components. J Mater Process Tech, 2008; 195: 282–298.

[2] Grujicic M, Sellappan V, Omar MA, Seyr N, Obieglo A, Erdmann M, Holzleitner J. An Overview of the Polymer-to-Metal Direct-Adhesion Hybrid Technologies for Load-Bearing Automotive Components. J Mater Process Tech, 2008; 197: 363–373.

[3] Grujicic M, Arakere G, Pisu P, Ayalew B, Seyr N, Erdmann M. Application of Topology, Size and Shape Optimization Methods in Polymer Metal Hybrid Structural Lightweight Engineering. Multidisc Model Mater Struc, 2008; 4: 305–330.

[4] Grujicic M, Sellappan V, Mears L, Xuan X, Seyr N, Erdmann M, Holzleitner J. Selection of the Spraying Technologies for Over-Coating of Metal-Stampings with Thermo-Plastics for Use In Direct-Adhesion Polymer Metal Hybrid Load-Bearing Component. J Mater Process Tech, 2008; 198: 300–312.

[5] Grujicic M, Pandurangan B, Bell WC, Daqaq M, Ma L, Seyr N, Erdmann M, Holzleitner J. A Computational Analysis and Suitability Assessment of Cold-Gas Dynamic Spraying of Glass-Fiber Reinforced Poly-Amide 6 for Use in Direct-Adhesion Polymer Metal Hybrid Automotive Components. Appl Surf Sci, 2008; 254: 2136–2145.

[6] Grujicic M, Sellappan V, Pandurangan B, Li G, Seyr N, Erdmann M, Holzleitner J. Computational Analysis of Injection-Molding Residual-Stress Development in Direct-Adhesion Polymer-to-Metal Hybrid Body-In-White Components. J Mater Process Tech, 2008; 203: 19–36.

[7] Grujicic M, Sellappan V, Arakere G, Seyr N, Obieglo A, Erdmann M, Holzleitner J. The Potential of a Clinch-Lock Polymer Metal Hybrid Technology for Use in Load-Bearing Automotive Components. J Mater Eng Perform, 2009; 18: 893–902.

[8] Grujicic M, Sellappan V, He T, Seyr N, Obieglo A, Erdmann M, Holzleitner J. Total Life-Cycle Based Materials Selection for Polymer Metal Hybrid Body-In-White Automotive Components. J Mater Eng Perform, 2009; 18: 111–128.

[9] Grujicic M, Sellappan V, Kotrika S, Arakere G, Obieglo A, Erdmann M, Holzleitner J. Suitability Analysis of a Polymer Metal Hybrid Technology Based on High-Strength Steels and Direct Polymer-to-Metal Adhesion for Use in Load-Bearing Automotive Body-In-White Applications. J Mater Process Tech, 2009; 209: 1877–1890.

[10] Grujicic M, Sellappan V, Arakere G, Ochterbeck JM, Seyr N, Obieglo A, Erdmann M, Holzleitner J. Investigation of a Polymer Metal Inter-locking Technology for use in Load-bearing Automotive Components. Multidiscip Model Mater Struc, 2010; 6(1): 23–44.

[11] Korson C, Stratton D. An Integrated Automotive Roof Module Concept: Plastic-Metal Hybrid and Polyurethane Composite Technology. Proceedings of the 5th SPE Annual Automotive Composites Conference; 2005 Sep 14 –15. Troy, MI. Newport, CT: Society of Plastics Engineers.

[12] Zoellner OJ, and Evans JA. Plastic-Metal Hybrid. A New Development in the Injection Molding Technology. Annual Technical Conference of the Society of Plastics Engineers; 2002; San Francisco, CA. Newport, CT: Society of Plastics Engineers. p1–4.

[13] Rosato D. 2007. Structurally Sound Plastic/Metal Hybrid Molding Emerging. Available at: http://www.omnexus.com/resources/editorials.aspx?id=16483. Accessed 2012 Aug 14.

[14] Leaversuch RD. 2003. Plastic-Metal Hybrids Make Headway On and Off the Road. Available at: http://www.ptonline.com/articles/plastic-metal-hybrids-make-headway-on-and-off-the-road. Accessed 2012 Aug 9.

[15] Recktenwald D. Advanced Adhesives Foster Hybrid Structures. Mach Des, 2005; 77(21): 124–126.

[16] Awaja F, Gilbert M, Kelly G, Fox B, Pigram PJ. Adhesion of polymers. Prog Polym Sci, 2009; 34: 948–968.

[17] Lucchetta G, Marinello F, Bariani PF. Aluminum sheet surface roughness correlation with adhesion in polymer metal hybrid overmolding. CIRP Ann–Manuf Techn, 2011; 60: 559–562.

[18] Grujicic M, Sellappan V, Arakere G, Seyr N, Erdmann M. Computational Feasibility Analysis of Direct-Adhesion Polymer-To-Metal Hybrid Technology for Load-Bearing Body-In-White Structural Components. J Mater Process Tech, 2008; 195: 282–298.

[19] Grujicic M, Sellappan V, Omar MA, Seyr N, Obieglo A, Erdmann M, Holzleitner J. An Overview of the Polymer-to-Metal Direct-Adhesion Hybrid Technologies for Load-Bearing Automotive Components. J Mater Process Tech, 2008; 197: 363–373.

[20] Ramani K, Moriarty B. Thermoplastic Bonding to Metals via Injection Molding for Macro-Composite Manufacture. Polym Eng Sci, 1998; 38: 870–877.

[21] Ramani K, Zhao W. The Evolution of Residual Stresses in Thermoplastic Bonding to Metals. Int J Adhes Adhes, 1997; 17(4): 353–357.

[22] Ramani K, Tagle J. Process-Induced Effects in Thin-Film Bonding of PEKEKK in Metal-Polymer Joints. Polym composite, 1996; 17(6): 879–886.

[23] Shah P. Adhesion of Injection Molded PVC to Silane Primed Steel [thesis]. Cincinnati (OH): University of Cincinnati; 2005.

[24] Sasaki H, Kobayashi I, Sai S, Omoto T, Mori K. Direct Adhesion of Nylon Resin to Stainless Steel Plates Coated with Triazine Thiol Polymer by Electropolymerization During Injection-Molding. Jpn J Poly Sci Tech, 1998; 55(8): 470–476.

[25] Erickson PW, Pleuddemann EP. Composite Materials 6. New York: Academic Press; 1974.

[26] Pleuddemann EP. Silane Coupling Agents. New York: Plenum-Press; 1991.

[27] Salladay J, Stevens J, *New Business Identification and Development*, Private Communication, October 2006.

[28] Berry DH, Namkanisorn A. Fracture Toughness of a Silane Coupled Polymer-Metal Interface: Silane Concentration Effects. J Adhesion, 2005; 81: 347–370.

[29] Mikulec M, "*Feasibility of Automotive Coatings Designed for Direct Adhesion to TPO Materials*," Annual Technical Conference of the Society of Plastics Engineers; 1997; Toronto. Newport, CT: Society of Plastics Engineers.

[30] Kondos CA, Kahle CF II. Basecoats with Direct Adhesion to TPO. SAE Technical Paper 980708, 1998. Published: February 23, 1998. DOI:10.4271/980708.

[31] Drummer D, Schmachtenberg E, Hülder G, Meister S. $MK^2$—A novel assembly injection molding process for the combination of functional metal surfaces with polymer structures. J Mater Process Tech, 2010; 210: 1852–1857.

[32] Marcus SA, inventor; Dow Chemical Company, assignee. Manufacture of Draw-Redraw Cans Using Steel Sheet Material Film Laminated or Extrusion Coated with a High Density Polyethylene Graft Co-polymer. US patent 4,452,375. 1984 June 5.

[33] Borges MF, Amancio-Filho ST, dos Santos JF, Strohaecker TR, Mazzaferro JAE. Development of computational models to predict the mechanical behavior of Friction Riveting joints. Comp Mater Sci, 2012; 54: 7–15.

[34] Moldflow Plastics Insight, Version 6.0, User Documentation. Moldflow Corporation. Framingham, MA, 2006.

[35] Kamal MR, Kenig S. The Injection Molding of Thermoplastics Part I. Theoretical Model. Polym Eng Sci, 1972;12: 294–301.

[36] Hieber CA, Shen SF. A Finite-element/Finite-difference Simulation of the Injection-molding Filling Process. J Non-Newton Fluid, 1980; 7: 1–32.

[37] Chiang HH, Hieber CA, Wang KK. A Unified Simulation of the Filling and Postfilling Stages in Injection Molding Part 1. Formulation. Polym Eng Sci, 1991; 31: 116–124.

[38] Kennedy P. Flow Analysis of Injection Molds. Munich: Hanser; 1995.

[39] Crochet MJ, Dupret F, Verleye V. Injection Molding. In: Flow and Rheology in Polymer Composites Manufacturing. S. G. Advani, editor. Amsterdam: Elsevier; 1994. p 415–461.

[40] Kietzmann CVL, Van Der Walt JP, Morsi YS. A Free-front tracking algorithm for a control-volume Hele-Shaw method. Int J Numer Meth Eng, 1998; 41: 253–269.

[41] Gupta M, Wang KK. Fibers orientation and Mechanical Properties of Short-fiber-reinforced Injection-molded Composites: Simulation and Experimental Results. Polym Composite, 1993; 14: 367–381.

[42] Walsh SF. Shrinkage and Warping Prediction for Injection Molded Components. J Reinf Plast Comp, 1993; 12: 769–777.

[43] Givler RC, Crochet MJ, Pipes RB. Numerical Predictions of Fibers orientation in Dilute Suspensions. J Compos Mater, 1983; 17: 330–343.

[44] Lipscomb GG II, Denn MM, Hur DU, Boger DV. The Flow of Fiber Suspensions in Complex Geometry. J Non-Newton Fluid, 1988; 26: 297–325.

[45] Rosenberg J, Denn MM, Keunings R. Simulation of Non-recirculating Flows of Dilute Fiber Suspensions. J Non-Newton Fluid, 1990; 37: 317–345.

[46] Zheng R. Boundary Element Methods for some Problems in Fluid Mechanics and Rheology [dissertation]. Sydney (Australia): University of Sydney; 1991.

[47] Phan-Thien N, Zheng R, Graham AL. The Flow of a Model Suspension Fluid past a Sphere. J Stat Phys, 1991; 62: 1173–1195.

[48] Phan-Thien N, Graham AL. A New Constitutive Model for Fiber Suspensions: Flow Past a Sphere. J Rheol, 1991; 30: 44–57.

[49] Altan MC, Güçeri Sİ, Pipes RB. Anisotropic Channel Flow of Fiber Suspensions. J Non-Newton Fluid, 1992; 42: 65–83.

[50] Tucker CL III. Flow Regimes for Fiber Suspensions in Narrow Gaps. J Non-Newton Fluid, 1991; 39: 239–268.

[51] Chiang HH, Hieber CA, Wang KK. A unified simulation of the filling and postfilling stages in injection molding. Part I: Formulation. Polym Eng Sci, 1991; 31: 116–124.

[52] Guell D, Lovalenti M. An examination of assumptions underlying the state of the art in injection molding modeling. Annual Technical Conference of the Society of Plastics Engineers; 1995; Boston. Newport, CT: Society of Plastics Engineers. p.728–732.

[53] Rezayat M, Burton TE. A Boundary-integral Formulation for Complex Three-Dimensional Geometries. Int J Numer Meth Eng, 1990; 29: 263–273.

[54] Folgar FP, Tucker CL. Orientation Behaviour of Fibers in Concentrated Suspensions. J Reinf Plast Comp, 1984; 3: 98–119.

[55] Fan XJ, Phan-Thien N, Zheng R. A Direct Simulation of Fiber Suspensions. J Non-Newton Fluid, 1998; 74: 113–136.

[56] Phan-Thien N, Zheng R. Macroscopic Modelling of the Evolution of Fibers orientation During Flow. In: Papathanasiou TD, Guell DC, editors. Flow-Induced Alignment in Composite Materials. Cambridge UK: Woodhead; 1997. p 77–106.

[57] Jeffery GB. The Motion of Ellipsoidal Particles Immersed in Viscous Fluid. P R Soc Lond A – Conta, 1922; 102: 161–179.

[58] Yamane Y, Kaneda Y, Doi M. Numerical Simulation of Semi-dilute Suspensions of Rodlike Particles in Shear Flow. J Non-Newton Fluid, 1994; 54: 405–421.

[59] Baaijens FPT. Calculation of Residual Stress in Injection Molded Products. Rheol Acta, 1991; 30: 284–299.

[60] K. M. B. Jansen. Residual Stresses in Quenched and Injection Molded Products. Int Polym Proc, 1994; 9: 82–89.

[61] Boitout F, Agassant JF, Vincent M. Elastic Calculation of Residual Stresses in Injection Molding: Influence of Mold Deformation and Pressure in the Liquid. Int Polym Proc, 1995; 10: 237–242.

[62] Titomanlio G, Jansen KMB. In-mold Shrinkage and Stress Prediction in Injection Molding. Polym Eng Sci, 1996; 36: 2041–2049.

[63] Zoetelief WF, Douven LFA, Ingen-Housz AJ. Residual Thermal Stresses in Injection Molded Products. Polym Eng Sci, 1996; 36: 1886–1896.

[64] L. Caspers, VIp, *An Integral Approach to the Simulation of Injection Molding* [dissertation]. Eindhoven (The Netherlands): Eindhoven University of Technology; 1996.

[65] Bushko WC, Stokes VK. Solidification of Thermoviscoelastic Melts Part 1. Formulation of Model Problem. Polym Eng Sci, 1995; 35: 351–364.

[66] Bushko WC, Stokes VK. Solidification of Thermoviscoelastic Melts Part 2. Effects of Processing Conditions on Shrinkage and Residual Stresses. Polym Eng Sci, 1996; 35: 365–383.

[67] Bushko WC, Stokes VK. Solidification of Thermoviscoelastic Melts. Part 3. Effects of Mold Surface Temperature Differences on Warping and Residual Stresses. Polym Eng Sci, 1996; 36: 322–335.

[68] Bushko WC, Stokes VK. Solidification of Thermoviscoelastic Melts. Part 4. Effects of Boundary Conditions on Shrinkage and Residual Stresses. Polym Eng Sci, 1996; 36: 658–675.

[69] Bird RB, Armstrong RC, Hassager O. Dynamics of Polymeric Liquids. Volume 1, Fluid Mechanics. 2nd ed., New York: Wiley; 1987.

[70] Tanner RI. Engineering Rheology. 2nd ed. London: Oxford Press; 1988.

[71] Ferry JD. Viscoelastic Properties of Polymers. 3rd ed. New York: Wiley; 1980.

[72] Papathanasiou TD, Guell DC, editors. Flow-induced Alignment in Composite Materials. Cambridge, UK: Woodhead; 1997.

[73] Schapery RA. Thermal Expansion Coefficients of Composite Materials Based on Energy Principles. J Compos Mater, 1968, 2: 380–404.

[74] Advani SG, Tucker CL III. The Use of Tensors to Describe and Predict Fibers orientation in Short Fiber Composites. J Rheol, 1987; 31: 751–784.

[75] Grujicic M, Sellappan V, Arakere G, Ziegert JC, Koçer FY Schmueser D. Multi-Disciplinary Design Optimization of a Composite Car Door for Structural Performance, NVH, Crashworthiness, Durability and Manufacturability. Multidisc Model Mater Struc, 2009; 5: 1–28.

[76] Grujicic M, Pandurangan B, d'Entremont BP, Yen C-F Cheeseman BA. The Role of Adhesive in the Ballistic/Structural Performance of Ceramic/Polymer-Matrix Composite Hybrid Armor. Mat Design, 2012; 41: 380–393.